

Raman and Rayleigh Calibrations of the LHD YAG Thomson Scattering

Ichihiro YAMADA, Kazumichi NARIHARA, Hiroshi HAYASHI, Hisamichi FUNABA
and LHD experimental group

National Institute for Fusion Science, Toki 509-5292, Japan

(Received 13 December 2006 / Accepted 29 March 2007)

We have carried out absolute calibrations of the LHD YAG Thomson scattering system by using Raman scattering and Rayleigh scattering in order to verify the applicability of Rayleigh calibration in the LHD Thomson scattering, and make a comparative study of Raman and Rayleigh calibrations. In the LHD Thomson scattering device, Rayleigh calibration is expected to give more reliable calibration factors. For the Rayleigh calibration, additional Rayleigh channel was installed into 20 polychromators. The other 124 polychromators without Rayleigh channel were calibrated by only Raman scattering. In the Raman calibration, pure gaseous nitrogen was introduced into the LHD vacuum vessel whereas the Rayleigh calibration was made by using air as target gas. The calibration factors obtained from the Raman and Rayleigh calibrations show good agreements. Uncertainties in the calibration factors obtained from the Raman and Rayleigh calibrations are discussed.

© 2007 The Japan Society of Plasma Science and Nuclear Fusion Research

Keywords: LHD, Thomson scattering, Raman scattering, Rayleigh scattering, absolute calibration

DOI: 10.1585/pfr.2.S1106

1. Introduction

Thomson scattering device is one of the most reliable diagnostics for the measurements of electron temperature and density profiles of fusion plasmas. To obtain absolute electron densities, the Thomson scattering device should be absolutely calibrated. The absolute calibrations using rotational Raman and Rayleigh scatterings from various gases have been proposed and applied [1, 2]. The Raman calibration may be more convenient because the wavelength shifts as Thomson scattering, then no special changes in the system and the apparatus settings are required. On the other hand, since Rayleigh scattering doesn't shift the wavelength, a polychromator must be equipped with a special wavelength channel for detecting unshifted Rayleigh scattered light, and very careful measurements are required to suppress strong stray light. These are disadvantages in Rayleigh calibration. Especially the latter will be a serious problem in many cases. However, Rayleigh calibration is expected to give more reliable calibration factors in the LHD Thomson scattering system [3, 4]. Raman and Rayleigh calibrations have such advantage and disadvantage. In this paper, we describe comparative study of Raman and Rayleigh calibration for the LHD TAG Thomson scattering system.

2. Raman Calibration

The experimental setup in Raman calibration is identical to that of Thomson scattering measurements except for that gaseous nitrogen fills the LHD vacuum vessel upto

author's e-mail: yamadai@nifs.ac.jp

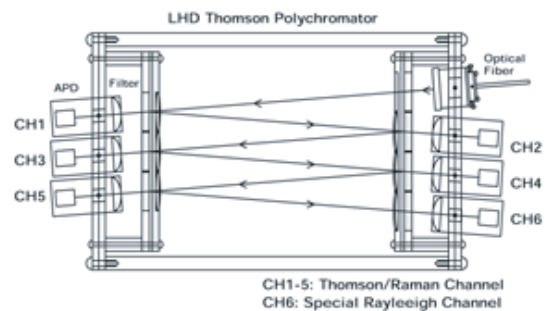


Fig. 1 Schematic diagram of the polychromator. Twenty polychromators have the sixth wavelength channel for Rayleigh calibration. The other 122 polychromators have five channels.

50 kPa, corresponding to the density of $1.3 \times 10^{19} \text{ m}^{-3}$. The LHD YAG Thomson scattering system is described in previous papers [3, 4]. The Thomson scattering uses several YAG lasers and Thomson scattered light is analyzed with 144 polychromators with five wavelength channels. 20 polychromators of them have also the sixth Rayleigh channel as shown in Fig. 1. Figure 2 shows effective Raman cross section and the spectral responsibilities of the channels 1, 2 and 6. The channel 6 is Rayleigh channel for Rayleigh calibration. The Raman cross section falls exponentially as wavelength shift increases, then the Raman signals can be detected by only channel 1 in the polychromators. Fundamental quantities of Raman scattering such as cross section and wavelength shift are summarized in

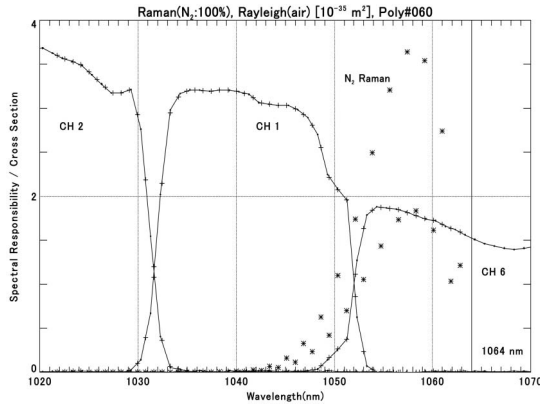


Fig. 2 Spectral responsibility of the channel 1, 2 and 6, and effective Raman cross section of molecular nitrogen.

the literatures [5–8]. Signal intensity of Raman scattered light detected by the channel 1, S_{Raman} , is given,

$$S_{Raman} = A_{Raman} \left[\sum_J w_J \sigma_J(\lambda_J) f_1(\lambda_J) \right] n$$

where A_{Raman} is the Raman calibration factor to be determined, n is the target gas density, J is the initial rotational quantum number, w_J is the population of the initial rotational state J , λ_J is the wavelength of the Raman shifted light, $\sigma_J(\lambda_J)$ is the Raman cross section for the $J \rightarrow J - 2$ transition, and $f_1(\lambda_J)$ is the spectral responsibility of the channel 1 at λ_J .

In Raman calibration,

$$k_{Raman} = A_{Raman} \left[\sum_J w_J \sigma_J(\lambda_J) f_1(\lambda_J) \right]$$

is obtained experimentally, and

$$\sum_J w_J \sigma_J(\lambda_J) f_1(\lambda_J)$$

is evaluated with some formulae on the Raman scattering. As shown in Fig. 2, overlap of the rotational Raman transition and spectral responsibility of the channel 1 is small in our polychromator, and $\sigma_J(\lambda_J) f_1(\lambda_J)$ is very sensitive to accuracy of wavelength of Raman scattering and the position and shape of the spectral responsibility. Figure 3 shows examples of an estimation of the error originated from the uncertainty of wavelength for some selected polychromators. As shown in the figure, even small uncertainty in wavelength may cause large error in the final results. This is the most troublesome disadvantage in the Raman calibration. The absolute wavelengths of the Raman transitions have been accurately established, however, the absolute position of the spectral responsibility may include some uncertainties. To decrease the uncertainties, we have carefully measured the spectral responsibility, and the temperatures of the polychromators have been stabilized with temperature-controlled, cooled water for suppressing the

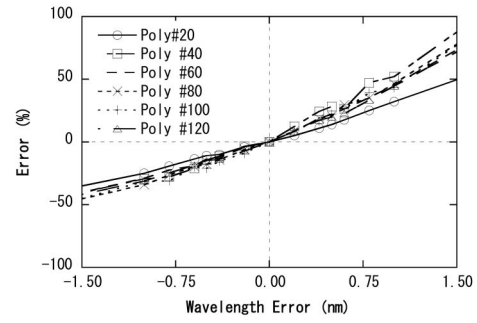


Fig. 3 Estimated error due to the uncertainty in the wavelength of Raman scattering and spectral responsibility.

variations of the filter characteristics. We have estimated the uncertainty to be ± 7 -10%. It is noted that angular distribution for quadrupole Raman transition differs from that of dipole Thomson scattering, and is nearly isotropic,

$$\frac{dI^{Raman}}{d\Omega} = \frac{3}{8\pi} \frac{6 + \sin^2 \beta}{10},$$

where β is the angle between the polarization vector of incident laser beam and observation direction.

3. Rayleigh Calibration

Fundamental procedure of Rayleigh calibration is the same as that of Raman calibration, except that the sixth Rayleigh channel is required for detecting unshifted Rayleigh scattered light, as shown in Figs. 1 and 2, and careful measures to eliminate strong stray light. In the Rayleigh calibration, the LHD vacuum vessel was filled with air upto 50 kPa. Rayleigh signal intensity detected by the channel 6, $S_{Rayleigh}$, is given by,

$$S_{Rayleigh} = A_{Rayleigh} \sigma_{Rayleigh} f_6(\lambda_{1064 \text{ nm}}) n,$$

where $A_{Rayleigh}$ is the Rayleigh calibration factor to be determined, n is the density of air, and $f_6(\lambda_{1064 \text{ nm}})$ is the spectral responsibility of the channel 6 at 1064 nm. Rayleigh calibration factor, $k_{Rayleigh} = A_{Rayleigh} \sigma_{Rayleigh} f_6(\lambda_{1064 \text{ m}})$ is obtained experimentally, and $\sigma_{Rayleigh} f_6(\lambda_{1064 \text{ m}})$ is evaluated with the Rayleigh cross section and the spectral responsibility of channel 6. In contrast to similar evaluation of

$$\sum_J w_J \sigma_J(\lambda_J) f_1(\lambda_J)$$

in Raman calibration, $\sigma_{Rayleigh} f_6(\lambda_{1064 \text{ m}})$ is mostly insensitive to the shape of spectral responsibility and then can be accurately determined by using a filter whose spectral responsibility is near flat-top at around 1064 nm. The error in determination of $\sigma_{Rayleigh} f_6(\lambda_{1064 \text{ m}})$ is estimated to be 1-2% or less, which is much smaller than that in the Raman calibration. We believe that this is a great advantage of Rayleigh calibration in the LHD Thomson scattering.

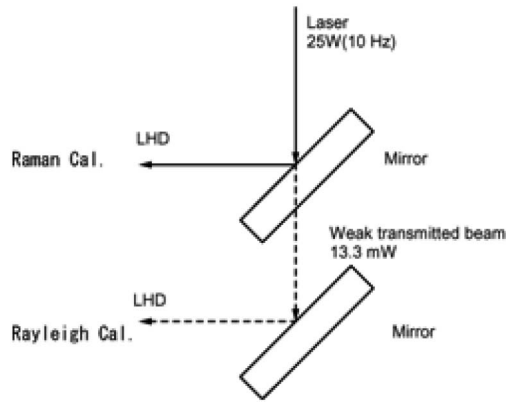


Fig. 4 Schematic diagram of the beam attenuation method in the Rayleigh calibration.

However, Rayleigh calibration will suffer from the strong stray light in many cases. We have solved the problem as follows. Rayleigh signal intensity, $S_{Rayleigh}$, is proportional to scattering cross section, $\sigma_{Rayleigh}$, target density, n , and laser intensity, L , whereas stray signal is proportional to laser intensity only,

$$S_{Rayleigh} \propto L(\sigma_{Rayleigh}n_{air}),$$

$$N_{Stray} \propto L.$$

Therefore, the stray light can be reduced by decreasing laser intensity. In the Rayleigh calibration, we decreased the laser intensity from 2.5 J/pulse to 1.33 mJ/pulse by a factor 5×10^{-5} by using a dielectric mirror as a beam attenuator. Figure 4 shows the schematics of the beam attenuation. Very weak transmitted light is introduced into the LHD vacuum chamber in the Rayleigh calibration, whereas full beam (2.5 J/pulse) is used in the Raman calibration. Even in such cases, since Rayleigh cross section is about 10^{3-4} times larger than effective Raman cross sections, both necessary scattering signal intensity and signal-to-background ratio can be obtained.

Figures 5 (a) and (b) show examples of target pressure dependence of scattering signals of Raman scattering and Rayleigh scattering respectively. Both of them show linear target pressure dependence as expected. The calibration factors are obtained from the gradients of the lines. Figure 6 shows the comparison of the calibration factors obtained from Raman and Rayleigh calibrations as the function of polychromator number. Both of the calibration factors show good agreements. Finally, we show an example of electron temperature and density profiles of LHD SDC plasmas in Fig. 7. The electron densities are absolutely calibrated with the Raman and Rayleigh factors obtained in this work. The results are consistent with other density relevant diagnostics in LHD.

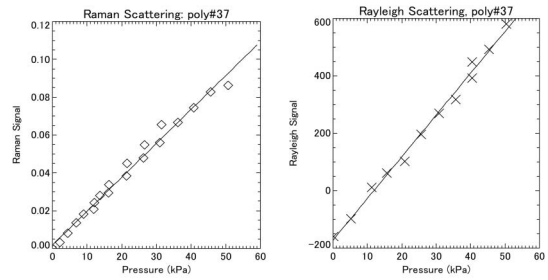


Fig. 5 Signal intensities of Raman, (a), and Rayleigh (b) scatterings as a function of target pressure. The calibration factors are determined from the gradient of the fit line.

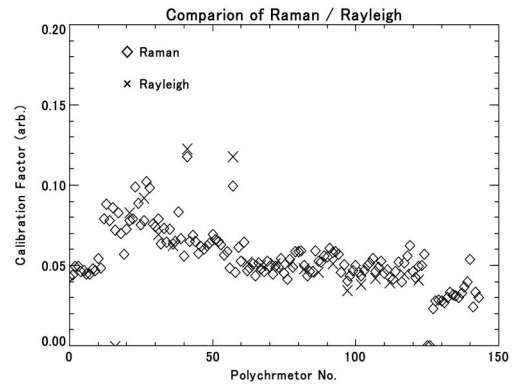


Fig. 6 Comparison of the calibration factors obtained from Raman and Rayleigh calibrations. They show good agreements.

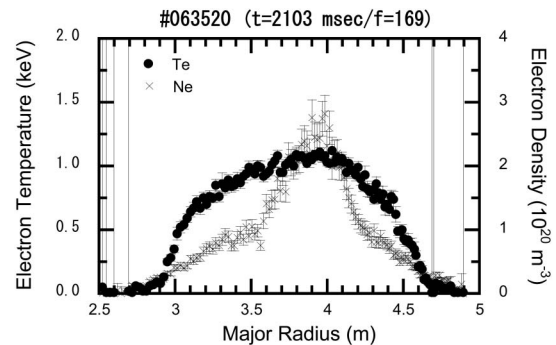


Fig. 7 An example of electron temperature and density profiles of LHD SDC plasmas. The electron density calibrated with the calibration factors obtained in this work.

4. Conclusions

We have carried out Raman and Rayleigh calibrations for the LHD YAG Thomson scattering system. We have verified that Rayleigh calibration is also practicable in the LHD Thomson scattering. The calibration factors obtained from the Raman and Rayleigh calibrations show good agreements. However, Rayleigh calibration may be suitable to the LHD YAG Thomson scattering because more

accurate calibration factors can be obtained. We are planning to equip all the polychromators with Rayleigh channels in order to carry out Rayleigh calibration for all polychromators.

Acknowledgements

This work was supported by the NIFS LHD project budget (NIFS05ULHH502 and NIFS06ULHH502), and partially supported by the Grant-in-Aid for Scientific Research (C), No. 16540456.

- [1] H. Röhr, Phys. Lett. **81**, 451 (1981).
- [2] J. Howard, B.W. James and W.I.B. Smith, J. Phys. D **12**, 1435 (1979).
- [3] K. Narihara *et al.*, Fusion Eng. Design **34-35**, 67 (1997).
- [4] K. Narihara, I. Yamada, H. Hayashi, and K. Yamauchi, Rev. Sci. Instrum. **72**, 1122 (2001).
- [5] C.M. Penny, R.L. St. Peters, and M. Lapp, J. Opt. Soc. Am. **64**, 712 (1974).
- [6] R.W. Carlson and W.R. Fenner, Astrophys. J. **178**, 551 (1972).
- [7] A. Weber, Raman Spectroscopy of Gases and Liquid (Springer-Verlag, Berlin, 1979) p.71.
- [8] I. Yamada *et al.*, Rev. Sci. Instrum. **74**, 1675 (2003).